Computational Materials Science 47 (2010) 934–939

Contents lists available at ScienceDirect

Computational Materials Science

journal homepage: www.elsevier.com/locate/commatsci

Structural properties of amorphous selenium: An *ab initio* molecular-dynamics simulation

J.A. Reyes-Retana *, Ariel A. Valladares

Instituto de Investigaciones en Materiales, Universidad Nacional Autónoma de México, Apartado Postal 70-360, México, DF 04510, Mexico

ARTICLE INFO

Article history:
Received 19 October 2009
Received in revised form 19 November 2009
Accepted 22 November 2009
Available online 16 December 2009

Keywords:
Amorphous selenium
ab initio molecular dynamics
Radial distribution functions

ABSTRACT

We use a new approach to generate amorphous selenium structures by an *ab initio* molecular dynamics method. We start with crystalline cubic supercells in a diamond-like structure with 64, 150 and 216 atoms, and with the experimental microscopic densities of $\rho = 0.0324$ (4.25 g cm^{-3}) and $\rho = 0.0340$ atoms Å^{-3} (4.45 g cm^{-3}). The samples are amorphized using DMol^3 from the suite in Material Studio 3.2® by heating the periodic structures to just below the melting point (the *undermelt-quench* approach) and then cooling them down to 0 K. The structures are relaxed by annealing and quenching, and finally a geometry optimization is carried out. We report radial distribution functions $g(r)$, bond angle distributions and dihedral angle distributions. We find that the amorphous structure, for both densities, is mainly formed by chains but not at all linear, there are some ring-like structure although not closed. Also the Radial Distributions Functions, RDFs, of Se have maxima at 2.35 Å and 3.75 Å for the first and second neighbors, respectively.

1. Introduction

The structure of amorphous selenium (a-Se) has been the subject of study for the last century and it continues being investigated. The earliest research on a-Se was oriented to apply it as an active layer in xerographic photocopying machines, furthermore, in recent years it has been used as a photoconductor for direct conversion in X-ray image detectors [1] and its application to Digital Mammography Systems [2]. Different experimental forms of producing amorphous selenium can be found: melt quenching [3–6], vapor deposition [3] and ball milling [7,8], where the structure of a-Se is reported as being chain-like, ring-like or both. In the experimental data recorded by Kaplow et al. [3], they reported that the vitreous selenium structure consist mainly of Se_8 rings. Henninger et al. [9] reported the existence of chains, but randomly oriented. And Jóvári et al. [8] suggest, *independent of the method of preparation*, that a-Se contains chain molecules of variable lengths, and that the dominance of Se_8 rings is improbable.

Some computer simulations have been carried out to understand the amorphous selenium structural properties. Hohl and Jones [10] used 64 atoms for their first-principles molecular-dynamics simulations and report the first and second neighbor peaks at 2.41 and 3.73 Å. Bichara et al. [11] were looking for the chain structure of a-Se using the tight-binding Monte Carlo (TB-MC) simulations with 648 atoms and they concluded that the fraction of twofold-coordinated atoms never exceeds 70%. Shimizu et al. [12] used 64, 216 and 512 atoms for their tight-binding molecular-dynamics simulations and they concluded that the first minimum of the radial distribution function (RDF) is in 2.75 Å and assumed that two atoms are bound if the distance between them is less than this value. From Fig. 1 of Ref. [12] the first and second peaks for a-Se are 2.24 and 3.50 Å. Zhang and Drabold [13] used 216 atoms for their *ab initio* molecular-dynamics simulations but they had significantly overestimated (about 6%) the value for the microscopic density according to Ref. [8]. From Fig. 1a of Ref. [13] the first and second peaks are: 2.39 and 3.75 Å. Hegedüs et al. determined how the structure changes occur due to the different preparation methods (liquid-quenching and evaporation) [14,15]. They used 1000 atoms with a classical empirical three-body potential of selenium to describe the interaction between atoms. They concluded that the upper limit of bond lengths is 2.8 Å and the first neighbor is located at 2.37 Å. They also concluded that samples prepared by rapid quenching are more homogeneous than the deposited ones. Recently, we have developed a thermal procedure (*undermelt-quench* approach [16]) to generate amorphous structures of pure and hydrogenated silicon [17], carbon [18], silicon–nitrogen [19] and carbon–nitrogen [20], and preliminary studies of silicon–germanium, indium–selenium and silicon–carbon have been carried out [21]. In the present study, amorphous structures of selenium are generated for 64, 150 and 216 atoms and the ring-like or chain-like structures are discussed.

* Corresponding author. Tel.: +52 55 56224622; fax: +52 55 56161251.
E-mail addresses: amorpho@gmail.com (J.A. Reyes-Retana), valladar@unam.mx (A.A. Valladares).
URL: http://www.iim.unam.mx/amorpho (J.A. Reyes-Retana).

0927-0256/$ - see front matter © 2009 Elsevier B.V. All rights reserved.
doi:10.1016/j.commatsci.2009.11.026

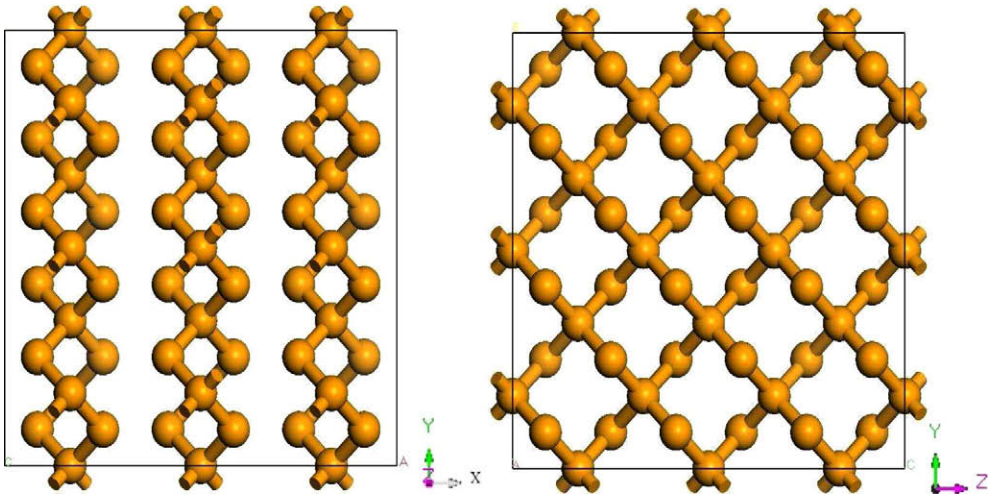

Fig. 1. Initial structure for 150 atoms. (a) Structure in the plane *XY* and the axis *Z* is out of the plane. (b) Structure in the plane *YZ* and the axis *X* is into the plane.

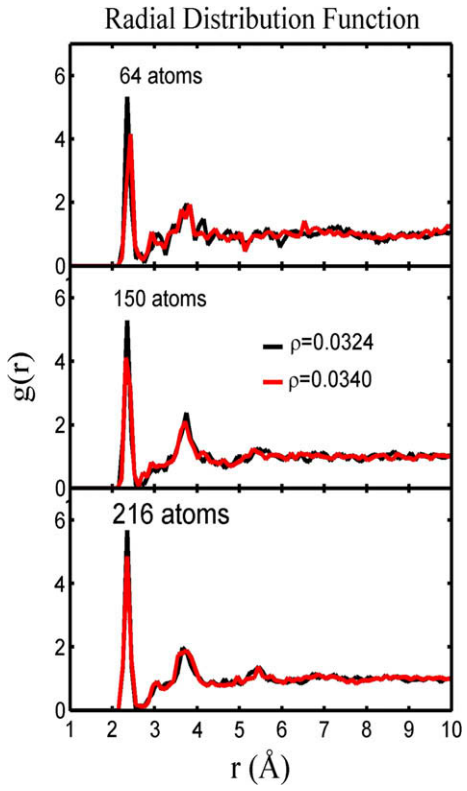

Fig. 2. Radial Distribution Functions for 64, 150 and 216 atoms. The black (dark) lines are those with density $\rho = 0.0324$ atoms Å^{-3} and the red (light) lines are those with density $\rho = 0.0340$ atoms Å^{-3}. (For interpretation of the references to color in this figure legend, the reader is referred to the web version of this article.)

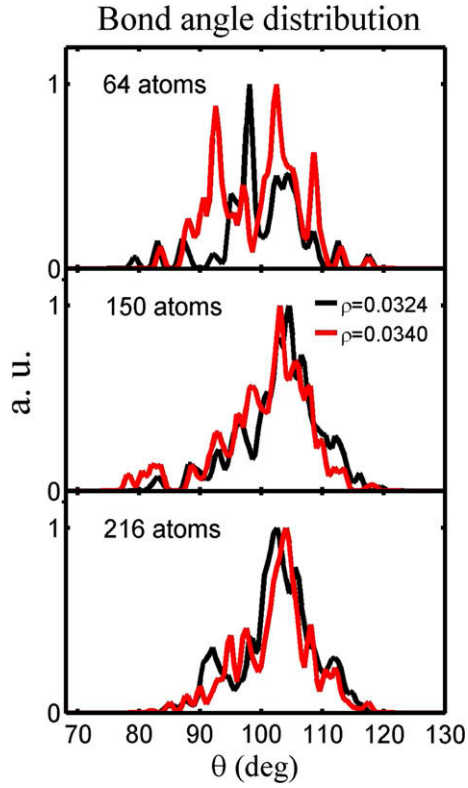

Fig. 3. Bond angle distributions for 64, 150 and 216 atoms. The black (dark) lines are those with density $\rho = 0.0324$ atoms Å^{-3} and the red (light) lines are those with density $\rho = 0.0340$ atoms Å^{-3}. (For interpretation of the references to color in this figure legend, the reader is referred to the web version of this article.)

Table 1
r_{max} is the maximum bond length, θ is the bond angle due to the first and second peaks, θ_{max} corresponds to the maximum value in the BAD and r_α are the distances of the small peak around 3 Å in the RDFs for 64, 150, 216 atoms and both densities.

Atoms	Density	r_{max} (Å)	$\theta = 2\sin^{-1}\left(\frac{r_2}{2r_1}\right)$ (°)	θ_{max} (°)	r_α (Å)
64	0.0324	2.750	105.9	98	3.05
	0.0340	2.73	104.2	102.5	2.93
150	0.0324	2.75	105.9	104	3.35
	0.0340	2.62	106.6	103	2.92
216	0.0324	2.55	101.9	100.5	3.05
	0.0340	2.75	105.9	104.5	3.05

2. Method

In previous simulations of selenium alloys [21], the Fast Structure code [22] was used; this code is found in the Cerius2® package and is based on the Harris functional [23]. In the Materials Studio® package, version 3.2, the option of simulated annealing in DMol^3 [24] has the Harris functional implemented. Both are DFT codes and they have integrated optimization techniques based on a fast force generator to allow simulated annealing molecular dynamics studies with quantum force calculations. The LDA parametrization

due to Vosko et al. [25] is used in both cases. The amorphization of the 64, 150 and 216 atoms were performed using DMol^3. In all cases the core is taken into account with a pseudopotential. The density functional semi-core pseudopotentials were generated by fitting all-electron relativistic DFT results, and for the amorphization process a double numerical basis set of atomic orbitals with polarization was chosen, with a cut-off of 5 Å in all cases. The default time step is given by $\sqrt{m_{min}/5}$, where m_{min} is the value of the mass in the system, selenium, and this leads to a time step of 3.97 fs. However, in order to increase the dynamical processes that occur in the amorphization and conclude it in reasonable computer time, a time step of 16 fs was used. The forces are calculated using rigorous formal derivatives of the expression for the energy in the Harris functional, as discussed by Lin and Harris [26].

One of the most important parameters in the modeling studies is the density. Two different densities were used in this study, the experimental one ($\rho_0 = 0.0324$ atoms Å^{-3} or 4.25 g cm^{-3}) [4] and the so called *correct* density suggested by Jóvarí and Pusztai (private communication) ($\rho_0 = 0.0340$ atoms Å^{-3} or 4.45 g cm^{-3}) [27]. The crystalline structures were amorphized with 64, 150 and 216 atoms with both densities mentioned above. In the case of 150 atoms, we started with a diamond structure but eliminated some atoms to have three planes of atoms, this was done in order to show that the initial structure does not affect the final amorphized structure (Fig. 1). All these simulations are done with periodic boundary conditions. The amorphization process is the following: all supercells are heated from 300 to 480 K, just below the melting point (494 K), in 100 steps of 16 fs each step, and

Table 2
The coordination percent is shown, and in the last column the ring distribution for 64, 150 and 216 atoms for both densities is listed.

Atoms	Density	Coordination (%)				Ring distribution
		$Z=1$	$Z=2$	$Z=3$	$Z=4$	
64	0.0324	1.56	84.38	14.06	0	No rings
	0.0340	9.38	78.12	12.50	0	No rings
150	0.0324	6.00	84.67	8.67	0.66	Two: 4-members and One: 7-members rings
	0.0340	10.00	80.00	10	0	One: 7-members ring
216	0.0324	10.18	81.48	8.34	0	One: 6-members rings
	0.0340	6.94	81.48	11.58	0	One : 5-members and One: 8-members rings

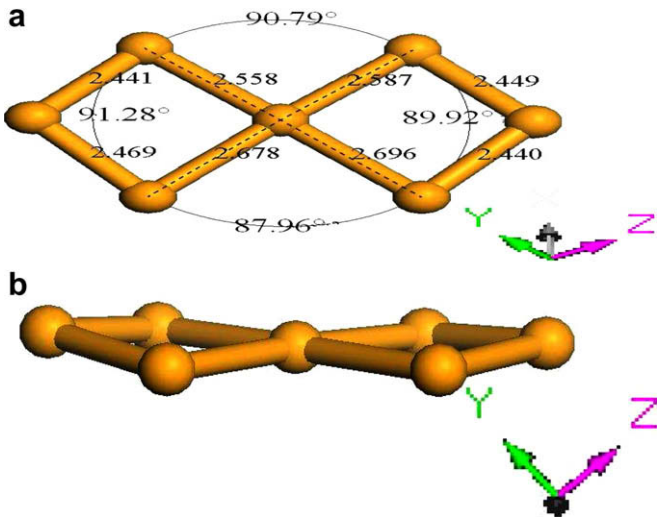

Fig. 4. Fourfold-coordinated atom: (a) showing the bond length (Å) and the bond angle, (b) the figure is rotated.

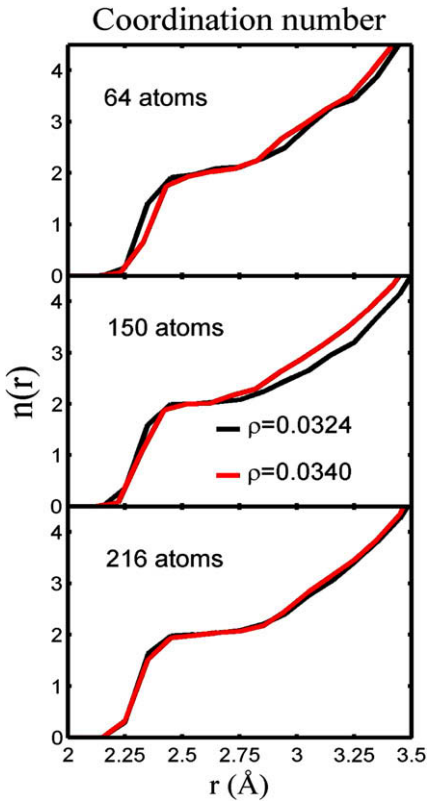

Fig. 5. Coordination number for 64, 150 and 216 atoms. The black (dark) lines are those with density $\rho = 0.0324$ atoms Å^{-3} and the red (light) lines are those with density $\rho = 0.0340$ atoms Å^{-3}. (For interpretation of the references to color in this figure legend, the reader is referred to the web version of this article.)

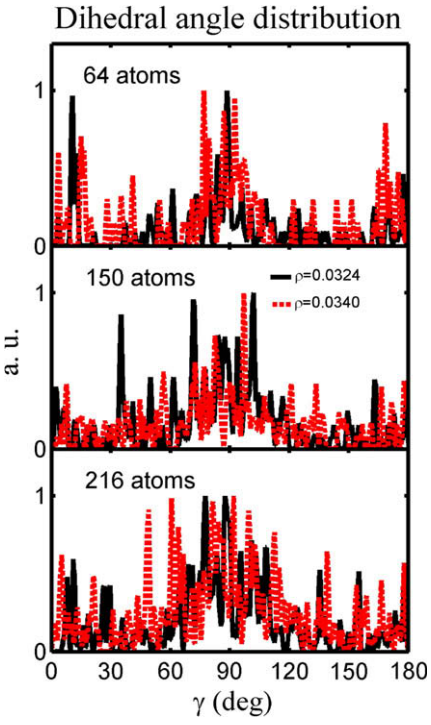

Fig. 6. Dihedral angle distributions for 64, 150 and 216 atoms. The solid (black) lines are those with density $\rho = 0.0324$ atoms Å^{-3} and the dashed (red) lines are those with density $\rho = 0.0340$ atoms Å^{-3}. (For interpretation of the references to color in this figure legend, the reader is referred to the web version of this article.)

immediately cooled down to 0 K in 266 steps. The heating/cooling rate was 0.113×10^{15} K/s. The atoms were allowed to move within each cell of volume $(12.5453\ \text{Å})^3$ and $(12.3472\ \text{Å})^3$ for 64 atoms, $(16.6643\ \text{Å})^3$ and $(16.4011\ \text{Å})^3$ for 150 atoms and $(18.8179\ \text{Å})^3$ and $(18.5208\ \text{Å})^3$ for 216 atoms with densities $\rho = 0.0324$ and $\rho = 0.0340$ respectively. Then all structures are subjected to annealing at 300 K and finally a quenching process. At the end, a geometry optimization was carried out to find the local energy minimum of the amorphous structures.

After this *undermelt-quench* approach, their topological properties were calculated, such as RDF, bond angle distribution (BAD), dihedral angle distribution (DAD) and the ring distribution frequency in each sample.

3. Results and discussion

The behavior of the RDFs is clearly smoother as the number of atoms increases. The RDFs are reported as $g(r) = \rho(r)/\rho_0$ and that is why it is convenient to use the microscopic density. In Fig. 2 it can be seen that the effect of the number of atoms, in molecular dynamics is to smooth the RDF. In this study, the RDFs are not artificially smoothed to show that first: even if few atoms are used (64), the results for the first and second neighbor are in good agreement with experiments [28]. The first and second neighbors for 64 atoms and densities $\rho = 0.0324$ and $\rho = 0.0340$ atoms Å^{-3} are: 2.35, 3.75 and 2.42, 3.82 Å respectively. The first and second neighbors for 150 atoms with the densities mentioned above are: 2.35, 3.75 and 2.32 and 3.72 Å respectively. And finally for 216 atoms the first and second neighbors with the densities mentioned above are: 2.35, 3.65 and 2.35 and 3.75 Å respectively. A knowledge of the first and second neighbors immediately gives a value for the bond angle θ [29]. The BADs were determined by defining the maximum bond length between two atoms as the first minimum (r_{max}) of the RDFs (see Table 1). If two atoms are bonded to a third one then the bond angle is calculated and the distribution is displayed in Fig. 3. For each sample the angle for the maximum in BAD (θ_{max}) is reported (Table 1) and compared with the theoretical bond angle due to the first and second neighbor.

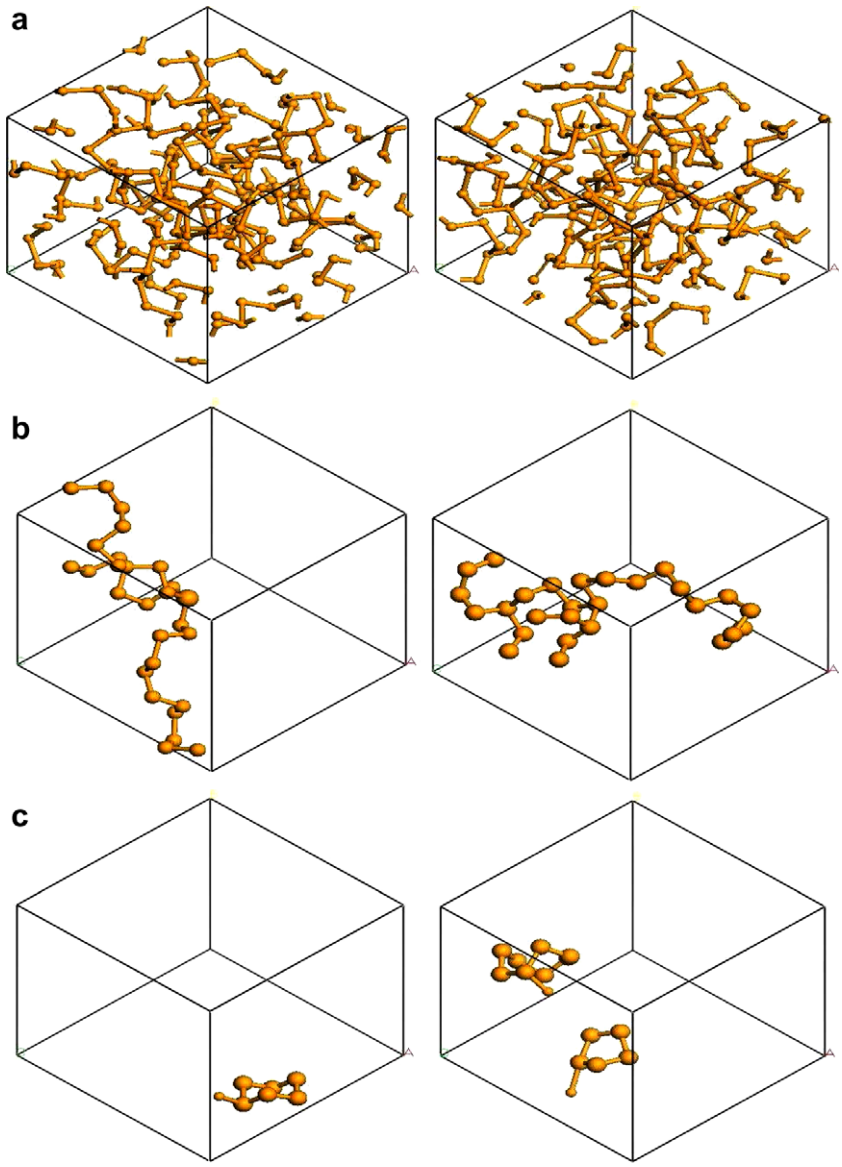

Fig. 7. (a) Amorphous structure of 216 atoms with $\rho = 0.0324$ atoms Å^{-3} left one and $\rho = 0.0340$ atoms Å^{-3} right one. (b) Largest chain. (c) Ring structures.

One of the most important results in this study is the presence of the small peak close to the 3.0 Å. We associate this peak to an allotropic form of selenium which is the α-cubic [30], this suggest that the a-Se presents some characteristics that are similar to the ones associated to α-cubic, namely the bond length r_α and the bond angle close to 90° [31]. A similar feature can be observed in scattering studies before applying the Hamming window to eliminate truncations errors [4]. r_α is the nearest neighbor distance in the α-cubic structure, 3.0 Å and it is shown in Table 1. Hohl and Jones [10] reported this feature as *threefold coordinated defects*, but if it is considered that the maximum bond length is the r_{max} then there exist some threefold defects just below the r_α, in fact, if the bond length is taken as r_α then the coordination number is greater than three.

The experimental results show that for crystalline Se the bond angle is 103.1 ± 0.2° and the dihedral angle is 100.7 ± 0.1° for the chain structure and the bond angle is 105.7 ± 1.6° and the average dihedral angle is 101.3 ± 3.2° for the ring structure [30]. The fraction of the twofold-coordinated atoms was calculated using r_{max}, see Table 2. In the sample of 150 atoms with ρ = 0.0324 atoms Å^{-3} there is a fourfold-coordinated atom that is shared at a corner by the two 4 member rings. Also these atoms present the characteristic bond angle around 90° [31], see Fig. 4. The coordination number is another manner to show the connectivity between selenium atoms (Fig. 5). The ring distribution was calculated and shown in Table 2. With the same criterion, if there is a chain of four atoms bonded, the dihedral angle is calculated and shown in Fig. 6. In the smaller samples (64 atoms) there are no rings, but the advantage of this approach, is the model's visualization. As the results show, the structure is mainly formed by chains (bond angle around 102° and dihedral angle around 100°) but there are some non-closed "rings". In the samples with 150 and 216, there are some rings in the structures (see Table 2), but once again, the results show, that the structures are mainly formed by chains, and some of these chains have atoms that look like non-closed "rings" (Fig. 8). Clearly the sample with 64 atoms does not seem to be large enough to allow the formation of the "rings" observed in the larger ones.

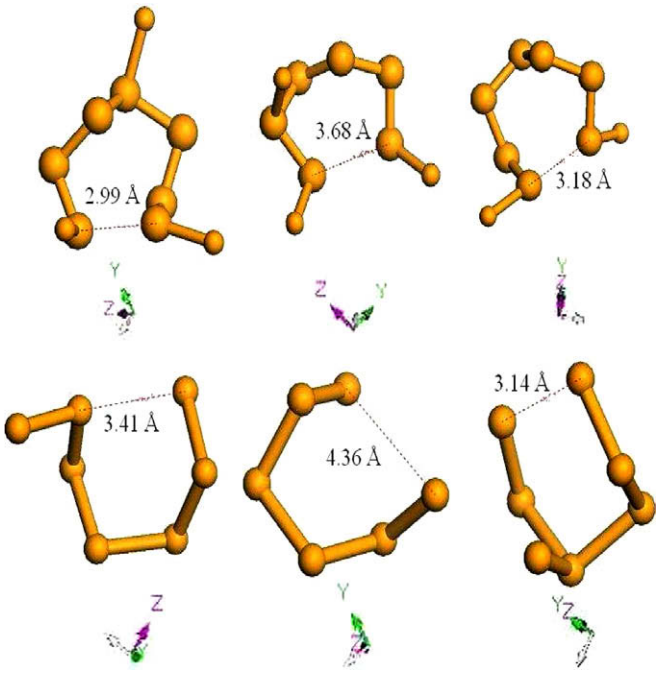

Fig. 8. Some non-closed rings in our simulations for $\rho = 0.0324$ atoms Å^{-3} at the top and $\rho = 0.0340$ atoms Å^{-3} at the bottom.

With respect to the density, it can be seen that as the supercell gets larger, the results of both densities tend to converge. For the 216 atoms samples the amorphous structures are shown, see Fig. 7. The largest chain in each structures was isolated, also the corresponding ring structure (see Table 2). In Fig. 8 some non-closed rings structures are shown, even though the amorphous structures are mainly formed by chains, it can be seen that there are only a few rings (one for $\rho = 0.0324$ and two for $\rho = 0.340$ atoms Å^{-3}) and some non-closed "rings".

4. Conclusions

We were able to generate, from first principles, random structures that have similar features and that are in qualitative agreement with the experiment [28]. This was done by a recently developed process, the *undermelt-quench* approach, which seems to work for DMol^3, using the Harris approximation. The results of these simulations reveal that the maximum of the Se–Se bond distribution is located at a distance of 2.35 Å . The results reported here indicate that a-Se with 64, 150, 216 atoms present a characteristic peak around 3 Å which correspond to an interatomic distance found in the crystalline α-cubic from. The a-Se structures are mainly formed by chains but there exists some rings and non-closed "rings" and structures in agreement with recent experimental findings [8]. The differences due to density tend to converge as the supercells grow. The fraction of the twofold-coordinated atoms is 80% on the average. Some of these defects affect directly the band gap of the vibrational density of states (to be published).

Acknowledgements

JARR acknowledges the financial support of CONACyT during his PhD studies. AAV is grateful to DGAPA-UNAM for funding his scientific Projects number IN101798, IN100500, IN119105 and IN119908. The calculations were carried out in the computer center of DGSCA-UNAM. M.T. Vázquez and O. Jiménez provided the information requested.

References

[1] G. Belev, S.O. Kasap, J. Non-Cryst. Solids 345 (2004) 484.
[2] M. Hoheisel, L. Bätz, T. Mertelmeier, J. Giersh, A. Korn, IEEE Trans. Nucl. Sci. 53 (2006) 1118.
[3] R. Kaplow, T.A. Rowe, B.L. Averbach, Phys. Rev. 168 (1968) 1068.
[4] F. Yssing Hansen, T. Steen Knudsen, K. Carneiro, J. Chem. Phys. 62 (1975) 1556.
[5] M. Inui, K. Maruyama, S. Takeda, S. Tamaki, Y. Waseda, J. Phys. Soc. Jpn. 63 (1994) 1378.
[6] R. Bruening, E. Irving, G. LeBlanc, J. Appl. Phys. 89 (2001) 3215.
[7] T. Fukunaga, M. Utsumi, H. Akatsuka, M. Misawa, U. Mizutani, J. Non-Cryst. Solids 205 (1996) 531.
[8] P. Jóvári, R.G. Delaplane, L. Pusztai, Phys. Rev. B 67 (2003) 172201.
[9] E.H. Henninger, R.C. Buschert, L. Halton, J. Chem. Phys. 46 (1967) 586.
[10] D. Hohl, R.O. Jones, J. Non-Cryst. Solids 117 (1990) 922; D. Hohl, R.O. Jones, Phys. Rev. B 43 (1991) 3856.
[11] C. Bichara, A. Pellegatti, J.-P. Gaspard, Phys. Rev. B 49 (1994) 6581.
[12] F. Shimizu, H. Kaburaki, T. Oda, Y. Hiwatari, J. Non-Cryst. Solids 250 (1999) 433.
[13] X. Zhang, D.A. Drabold, Phys. Rev. Lett. 83 (1999) 5042.
[14] J. Hegedüs, K. Kohary, S. Kugler, J. Non-Cryst. Solids 338-340 (2004) 283.
[15] J. Hegedüs, S. Kugler, J. Optoelectron. Adv. Mater. 7 (2005) 1923.
[16] Ariel A. Valladares, A new approach to the ab initio generation of amorphous semiconductors structures. Electronic and vibrational studies, in: Jonas C. Wolf, Luka Lange (Eds.), Glass Materials Research Progress, Nova Science Publisher, 2008, pp. 61–123.
[17] A.A. Valladares, F. Alvarez, Z. Liu, J. Stitch, J. Harris, Eur. Phys. J. B 22 (2001) 443.
[18] F. Alvarez, C.C. Díaz, R.M. Valladares, A.A. Valladares, Diam. Relat. Mater. 11 (2002) 1015.
[19] F. Alvarez, A.A. Valladares, Phys. Rev. B 68 (2003) 205203; F. Alvarez, A.A. Valladares, Solid State Commun. 127 (2003) 483.
[20] A.A. Valladares, F. Alvarez-Ramirez, Phys. Rev. B 73 (2006) 024206.
[21] Y. Peña, M. Mejía, J.A. Reyes, R.M. Valladares, Fernando Alvarez, A.A. Valladares, J. Non-Cryst. Solids 338–340 (2004) 258.

[22] FastStructure_SimAnn User Guide, Release 4.0.0, Molecular Simulations, Inc., San Diego, September 1996.
[23] J. Harris, Phys. Rev. B 31 (1985) 1770.
[24] B. Delley, J. Chem. Phys. 92 (1990) 508;
B. Delley, J. Chem. Phys. 113 (2000) 7756 (DMol^3 is implemented in the Materials Studio Suite®).
[25] S.H. Vosko, L. Wilk, M. Nusair, Can. J. Phys. 58 (1980) 1200.
[26] Z. Lin, J. Harris, J. Phys. Condens. Matter 4 (1992) 1055.
[27] P. Jóvarí, L. Pusztai, Phys. Rev. B 64 (2001) 014205.
[28] R. Bellissent, Nucl. Instrum. Methods 199 (1982) 289.
[29] S.R. Elliot, Physics of Amorphous Materials, 2nd ed., Longman Scientific and Technical, England, 1990. pp. 74–75.
[30] M.A. Popescu, Non-Crystalline Chalcogenides, Kluwer Academic Publishers, London, 2000. pp. 9–11.
[31] A. Popov, Atomic structure and structural modification of glass, in: R. Fairman, B. Ushkov (Eds.), Semiconducting Chalcogenide Glass, Vol. I, Elsevier Academic Press, New York, 2004, p. 68.